water

Article

Land Subsidence Due to Groundwater Exploitation in Unconfined Aquifers: Experimental and Numerical Assessment with Computational Fluid Dynamics

Dayana Carolina Chalá [1], Edgar Quiñones-Bolaños [1] and Mehrab Mehrvar [2,*]

Presenter : Tzu-Hsin Wang

Advisor : Professor Shih-Jung Wang

Date : 2025/05/09

- The potential global exposure to **land subsidence** according to Herrera-García et al. (2021) estimated a total of 31 countries happened subsidence in 2021 and will up to 85 countries in 2040.
- This pressing situation asks for further investigations to **prevent and manage** land subsidence, especially when it is related to the exploitation of unconfined aquifers in coastal regions and threatens the freshwater supply.

Literature Review

Table 1. Aquifers affected by land subsidence.

Aquifers and Study Area	Geological Characteristics [a]	Groundwater Exploitation Total or per Year	Data Collection	Type of Simulation	Maximum Subsidence
Chicot and Evangeline aquifer units (USA)	He, L, UNCO	5 m/year	Time series and InSAR	-	49 mm/year
Lower Bengal Delta (Bangladesh)	H, He, L, UNCO	5 m	Numerical simulation	Transient with MODFLOW	63 mm/year
Aguascalientes Valley (Mexico)	H, UNCO, Faults, R	3.5 m/year	SBAS InSAR	Fast Fourier Transform	120 mm/year
Morelia (Mexico)	H, UNCO, Faults, R	15 m/year	InSAR, settlement data	-	90 mm/year
Willcox Basin (Arizona)	He, L, CO	6 m/year Aprox.	InSAR, Hydraulic data	Storage loss estimation	140 mm/year
Wuxi City (China)	He, L, UNCO, CO	68 m	Extensometer	-	41.95 mm/year
Guangming Village (China)	He, L, UNCO, Faults, R	1 m	Experimental setup	Finite Element –Interfaced Elements	2–5 mm
Capo Colonna (Italy)	He, UNCO, Faults	-	InSAR, Geohazard Exploitation Platform	-	47 mm/year
Pingdu District (China)	H, UNCO	2400 mL/min	Experimental set up	-	0.708 mm
Chandigarh tri-city (India)	He, L, CO	0.2 m/year	InSAR, Field data	Neural network	8 mm/year
Bohai Bay (China)	He, L, CO	1.7×10^7 m^3/year	InSAR, Field data	Neural network	80–150 mm/year
Fuhuayuan (FHY) deep foundation pit project	He, L, CO	0.24 m/year	Experimental set up	DEM–CFD	8.7 mm
Yangtze River Delta (China)	He, L, UNCO, CO	0.75 m/year	Experimental setup	-	7–10 mm
Xuwei area (China)	He, L, UNCO, CO	2.34 mm/month	Experimental setup	-	14.04 mm
Hypothetical aquifer	H, UNCO	Cycles of 27% exploitation and recharge	Experimental setup	CFD	2–4 mm

This study

Notes: [a] He: Heterogeneous aquifer, H: Homogeneous aquifer, L: Layered aquifer, Faults: Aquifer with evidenced faults, UNCO: Unconfined aquifer, CO: Confined aquifer, R: Analyzed recharge rates.

Objective :

- To overcome the limitations of large-scale field studies and conventional numerical models, this study suggests the **experimental** recreation of land subsidence in a laboratory-scale setup subjected to exploitation and recharge.
- Use the **Computational Fluid Dynamics (CFD) model** to estimate aquifer compaction.

Background - Mathematical Modeling of Land Subsidence

There are mainly two approaches in the mathematical modeling of land subsidence :

1. **Terzaghi's law**

   Considers land subsidence as the **vertical displacement** resulting from compaction of the confining layers induced by water pressure variation.

2. **Biot's approach**

   Considers the land subsidence as a two- or three-dimensional problem, analyzing the **consolidation** of the soil and its **vertical and horizontal movement** due to water pressure changes and strain distribution.

Experimental Setup

Sandbox size :

2.70 m (length) × 1.25 m (height) × 0.10 m (width)

7 : porous media for packing sand

3、10 : area for observing water level

4、9 : screen mesh No.200 (0.074 mm)

2、11 : to control the water level

8 : vertical displacement sensors

1、14 : water reservoir

5、13 : pump

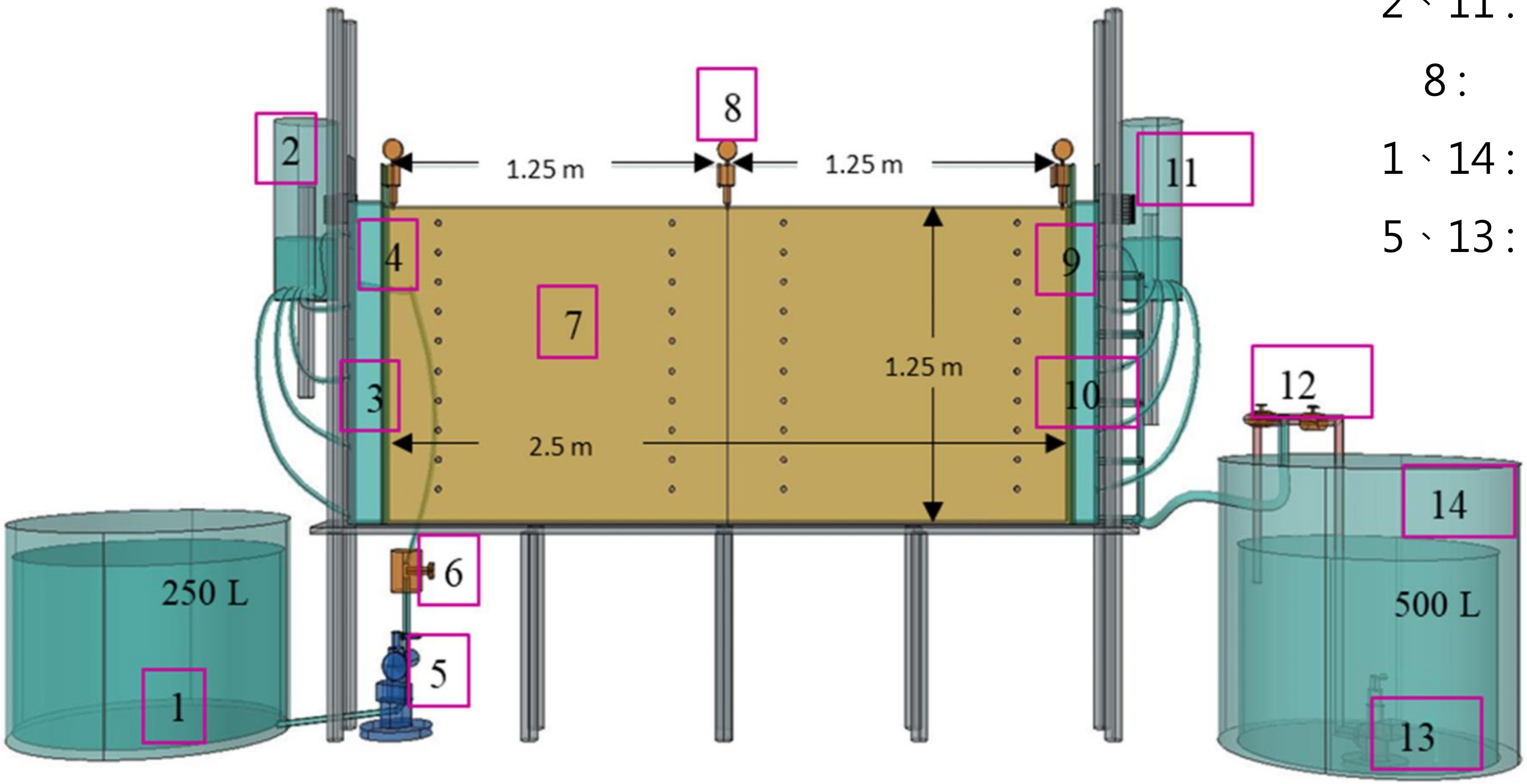

- 0.39 mm fine sand
- 0.67 mm coarse sand

Experimental Procedure

1. **Packing the sand with water**

   Filling 0.1 m of water, then adding 0.1 m of sand, repeated until the soil reached 1.1 m.

2. **Exploitation & Recharge Cycles**

   The initial hydraulic head was set to height of 1.1 m.

   Exploitation : lowering the water level to 0.8 m, this level was maintained for 24 hours.

   Recharge : increasing the water level to 1.1 m.

3. **Measuring Subsidence**

   One data every 24 hours.

Numerical Modeling of Land Subsidence

- COMSOL Multiphysics 6.0
- Assumptions of one-dimensional compaction and no additional sources of stress
- Estimation of the aquifer **vertical displacement** η :

Describes unsteady-state (one-dimensional) groundwater flow

$$\boxed{\frac{\partial}{\partial y}\left(K\frac{\partial h}{\partial y}\right) = S_h \frac{\partial h}{\partial t}}$$

K : hydraulic conductivity in the vertical axis

$\frac{\partial h}{\partial y}$: hydraulic head in the vertical axis

S_h : specific storage

$\frac{\partial h}{\partial t}$: hydraulic head over time

A simplified version derived from Terzaghi's Equation

$$\boxed{\eta = S_h b(-h)}$$

b : vertical thickness of aquifer sediments

h : hydraulic head

Boundary Conditions

- Top and bottom : no-flow.
- Lateral : head-controlled, with a change of the hydraulic head over time.

Parameters Considered for the Simulation

Table 2. Parameters for the numerical simulation.

Variable	Description	Value
ρ	Fluid density	1000 kg/m^3
p	Fluid pressure	0 Pa
$h(0)$	Initial hydraulic head	1.1 m
$h(t)$	Hydraulic head over time	$f(t)$

Table 3. Physical and mechanical properties of the sands.

Sand Type	Specific Gravity, *Gs*	Effective Diameter (mm)	Porosity (%)	Hydraulic Conductivity, *K* (m/s)
Fine sand	2.65	0.39	43.3	2×10^{-4}
Coarse sand	2.74	0.67	48.8	6.5×10^{-4}

Experimental Results - Coarse Sand

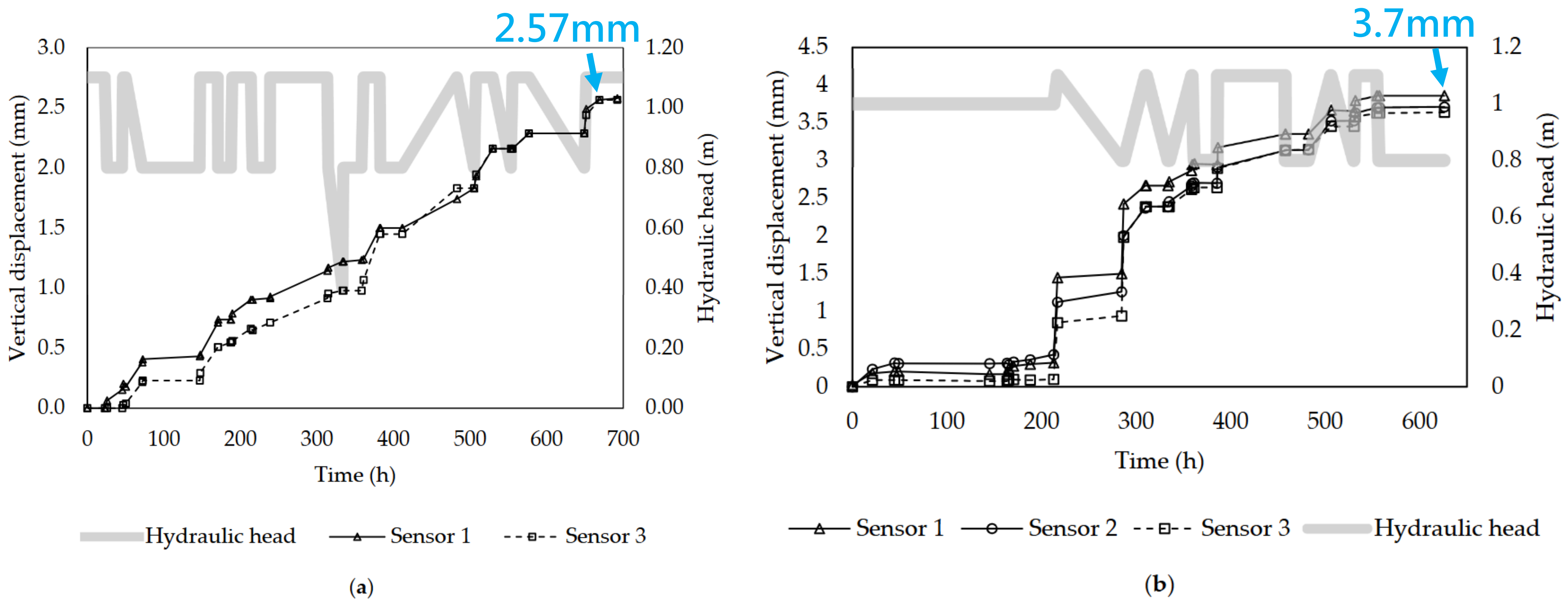

Figure 5. Variation of water table and vertical deformation in coarse sand. (**a**) The first scenario and (**b**) second scenario of coarse sand.

Repeated recharge & exploitation cycles → Hydraulic head changed → Pore pressure changed → Effective stress changed → Compaction of sand layers → Increased vertical displacement

~~ Terzaghi's law

Experimental Results - Fine Sand

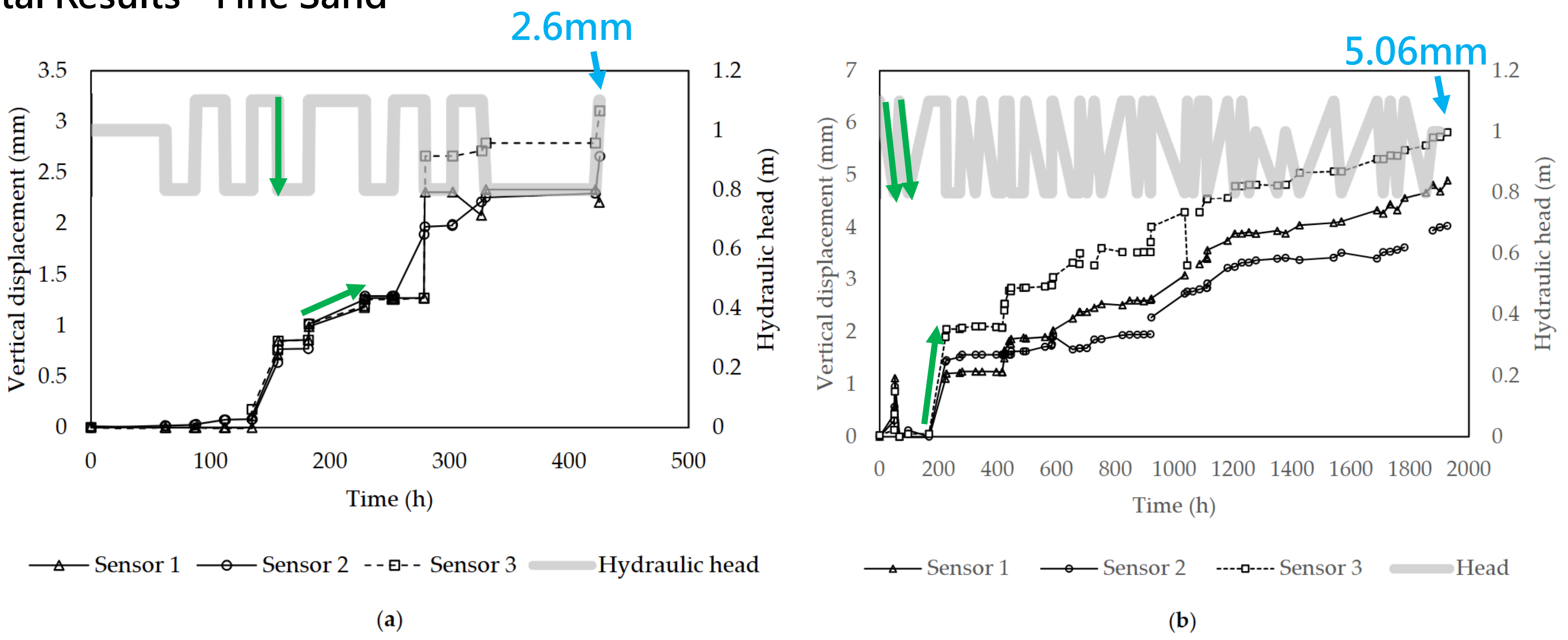

Figure 8. Variation of the water table and vertical deformation for fine sand type 30–40 for the (**a**) first scenario and (**b**) second scenario of fine sand.

- **Slower response** of the vertical deformation after the exploitation

Water Table different in Fine Sand and Coarse Sand

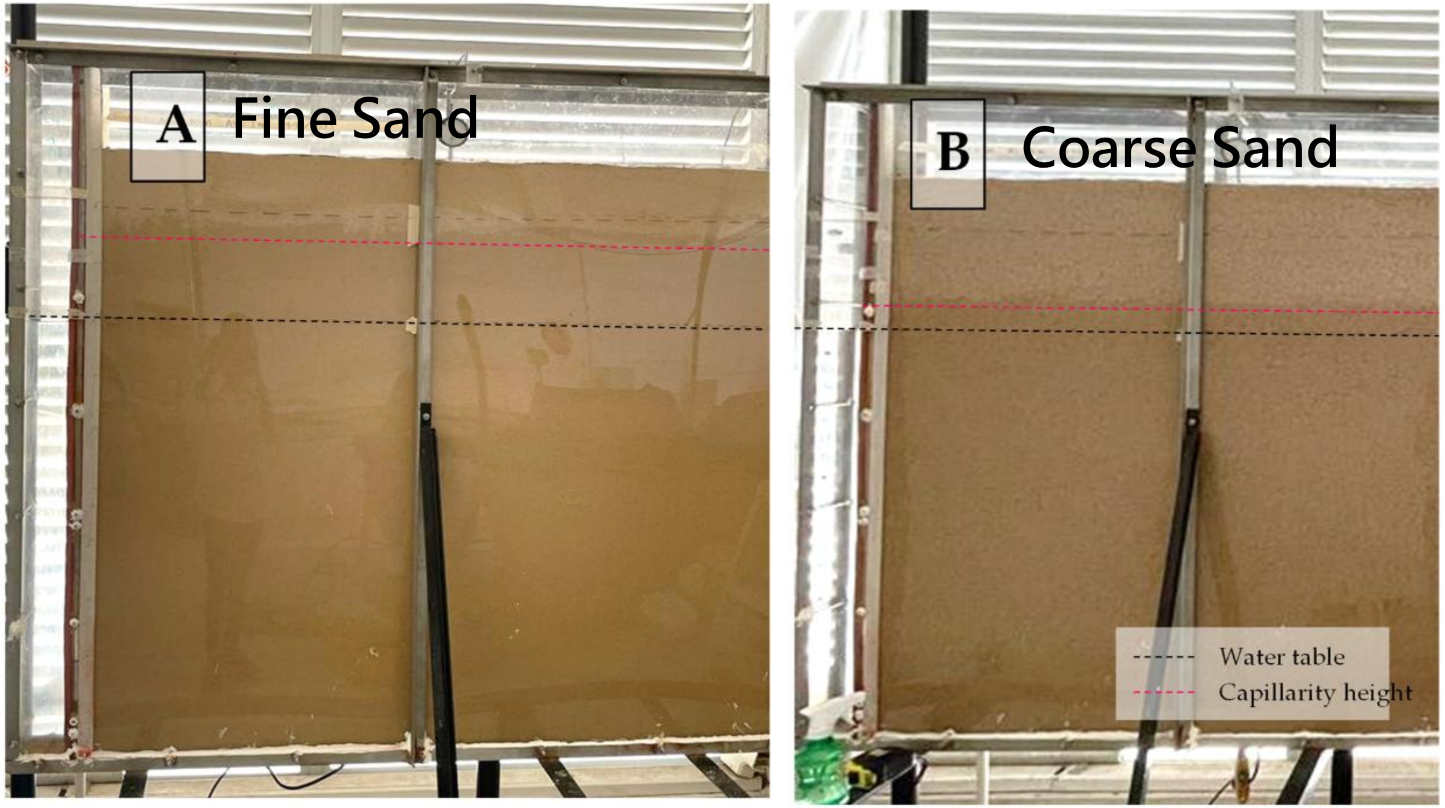

Figure 7. Water table of 0.8 m in (**A**) fine sand and (**B**) coarse sand.

The **capillary fringe** occurs when a percentage of saturation is trapped in the micropores of the sand, depending on **whether the porosity is high or low**.

Finer sands : porosity ↓ , capillary force ↑ , slower response

Numerical Results - Coarse Sand

S (specific storage) is the calibration parameter

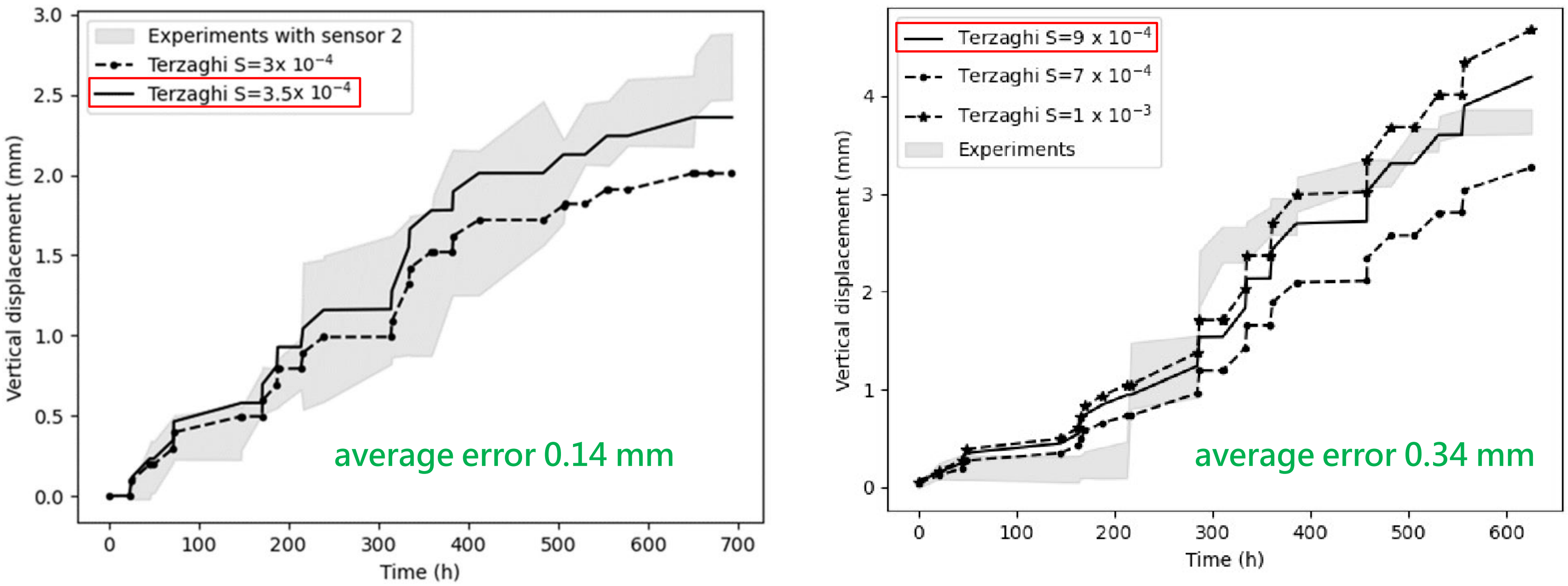

(**a**) First scenario (**b**) Second scenario

Figure 11. Vertical displacement in the coarse sand for the (**a**) first and (**b**) second scenario.

- Most simulation results fall within the experimental confidence interval, indicating **good predictive capability** of the model.
- For coarse sand shows a constant trend of increasing vertical displacement; over time, the slope started to decrease with the continued cycles of exploitation.

Numerical Results - Fine Sand

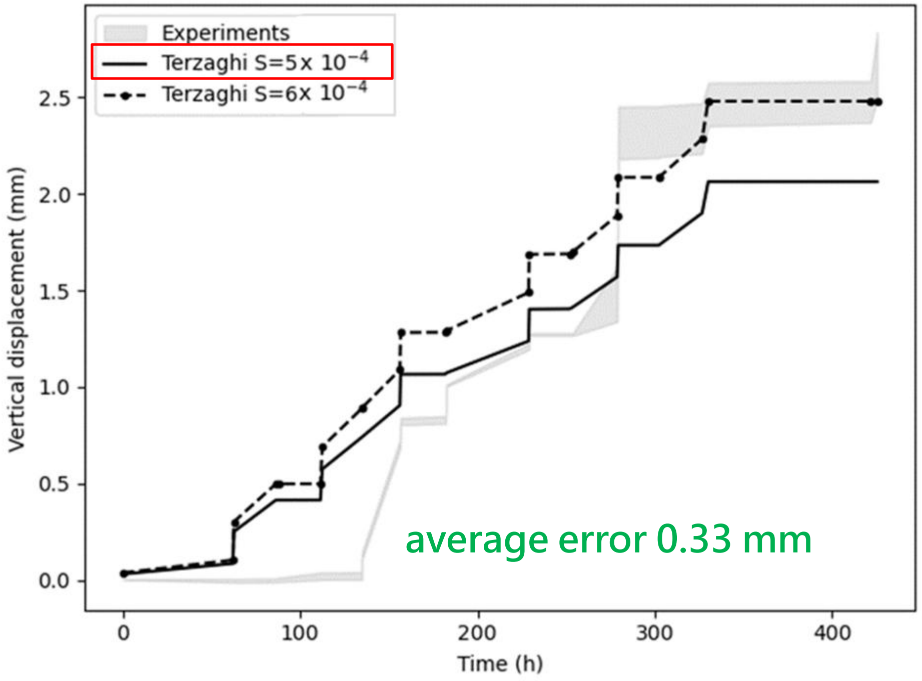

(a) First scenario

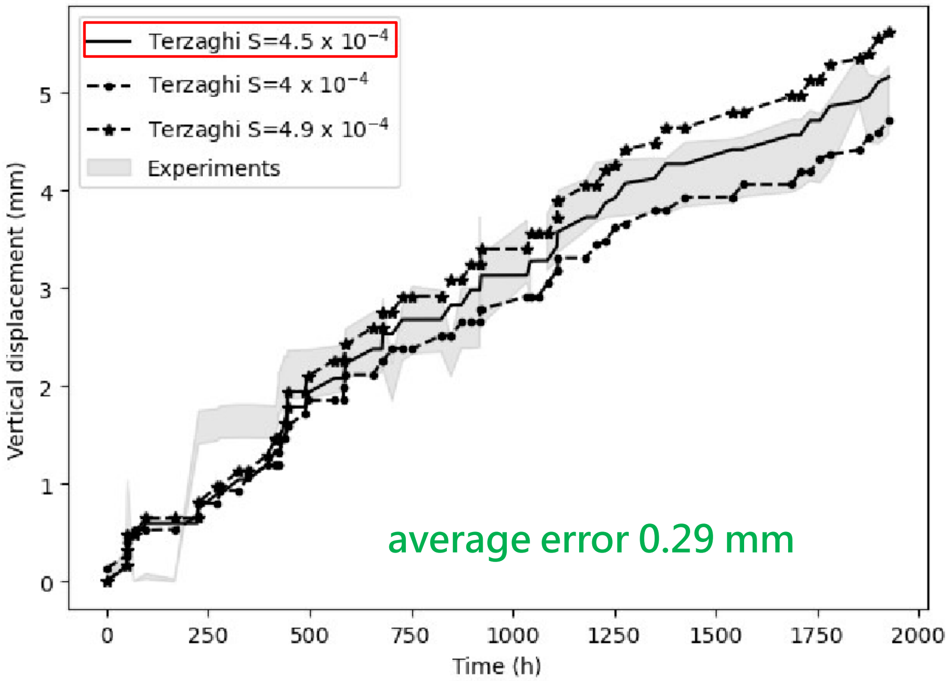

(b) Second scenario

Figure 12. Vertical displacement in the fine sand for the (**a**) first and the (**b**) second scenario.

- The agreement between the experimental and numerical results shows the potential of the CFD model to simulate land subsidence.
- The second scenario lasted more than **three months** and the simulation recreated the trend of vertical deformation observed in the experiments.

The novelty of this study is the estimation of land subsidence based on Terzaghi's approach using CFD model, and the simulation of scenarios of land subsidence for up to three months in coarse and fine sands using an experimental setup.

1. During the continued cycles of recharge and exploitation, both sands showed **continued compaction** over time. However, the deformation of coarse sand occurred at higher rates than fine sand, and **fine sands showed a delayed response**.
2. The estimation of land subsidence following Terzaghi's approach agreed with the vertical displacement behavior in lab data.
3. The experimental results show that in addition to the **specific storage** that contributes to deformation, fine and coarse sands showed a different response to **capillarity effects** due to their different **grain size and porosity**.

Thanks for your listening

- the water table is in a constant state and the hydrostatic stress and geostatic stress are not altered, showing a constant effective stress (σ')
- after the water exploitation occurs, and the hydrostatic stress is lowered, changing the geostatic stress, and increasing the effective stress.

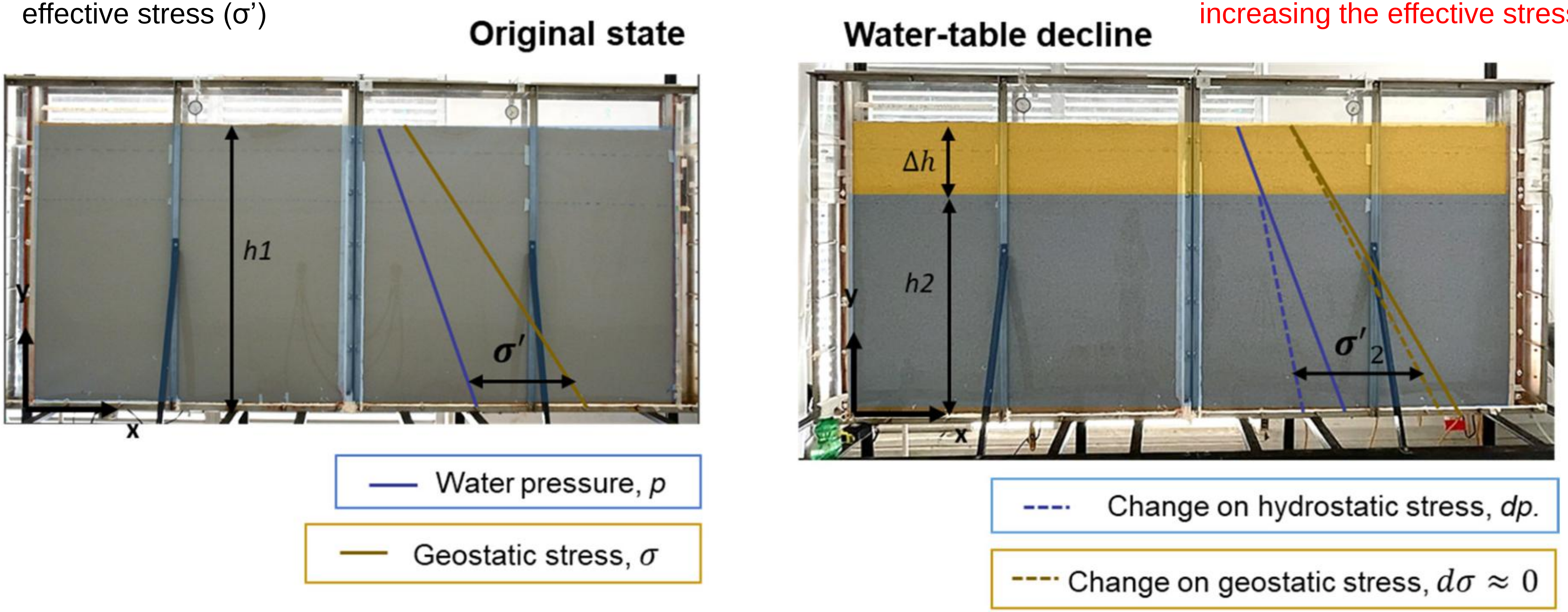

Figure 1. Stress diagrams for the water table decline in an unconfined aquifer.

Background - Groundwater Flow Equations

$$\boxed{\nabla\cdot(-K(\nabla h)) = S_h \frac{\partial h}{\partial t}}$$

K : hydraulic conductivity

h : hydraulic head

S_h : specific storage

The relationship between strain and stress is estimated with the measurements of the change on the **hydraulic head** after each cycle of **recharge and exploitation** of water.

The **variation of the effective stress ($\Delta\sigma'$)** with the hydraulic head change :

$$\boxed{\Delta\sigma' = (\Delta\sigma'_1 \cdot \Delta h + \Delta\sigma'_2 \cdot h_2) / (\Delta h + h_2)}$$

h_2 : water table depth after withdrawal

Considering the exploitation and recharge cycles :

$$\Delta\sigma' = \frac{\gamma\cdot\Delta h + \Delta\sigma'_2\cdot h_2}{(\Delta h + h_2)} \text{ withdrawal}$$

$$\Delta\sigma' = \frac{-\gamma\cdot\Delta h + \Delta\sigma'_2\cdot h_2}{(\Delta h + h_2)} \text{ recharge}$$

γ : unit weight of water

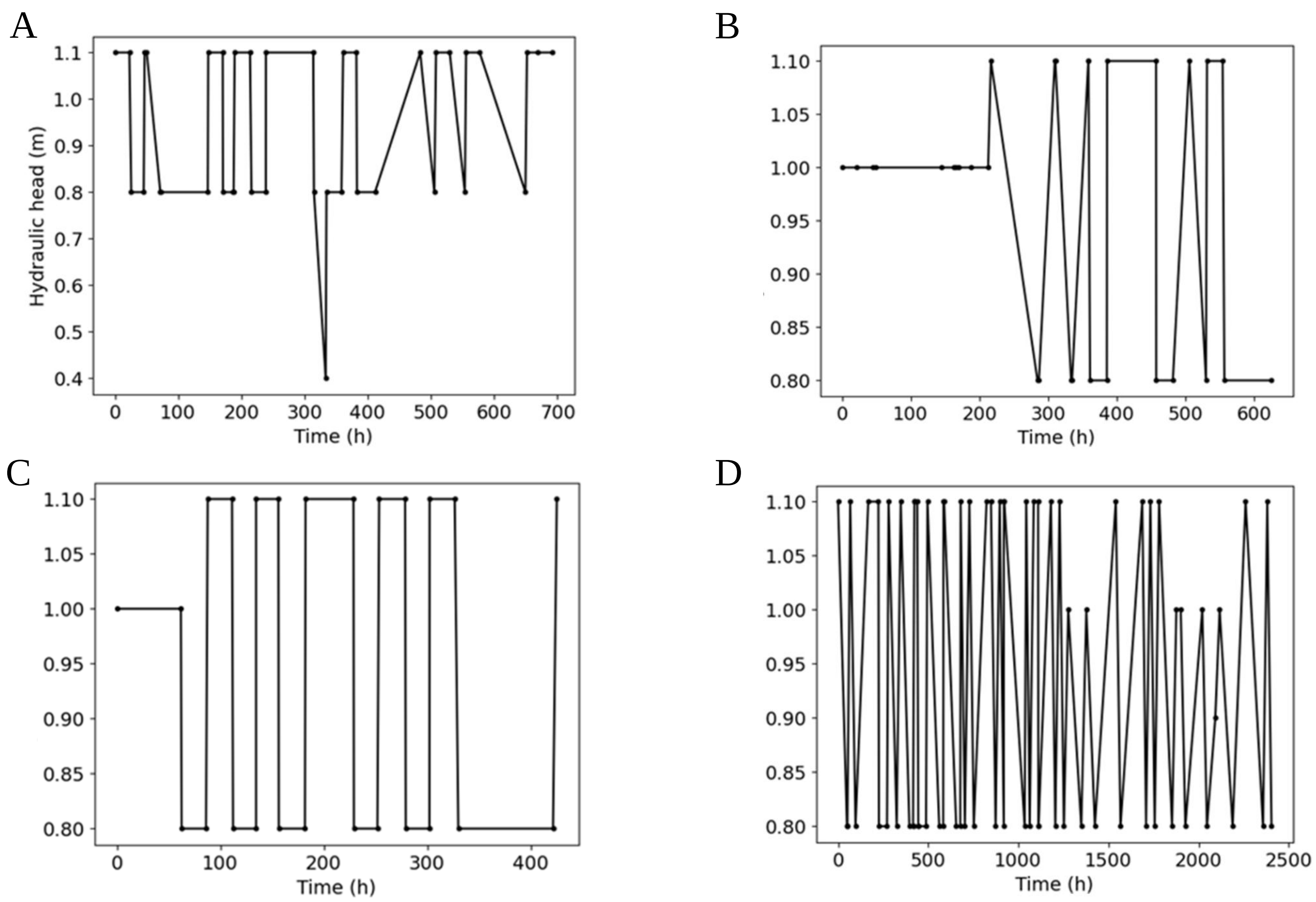

Figure 3. Hydraulic head over time for the cycles of recharge and exploitation. (**A**) First scenario of coarse sand, (**B**) Second scenario of coarse sand, (**C**) First scenario of fine sand, and (**D**) Second scenario of fine sand.

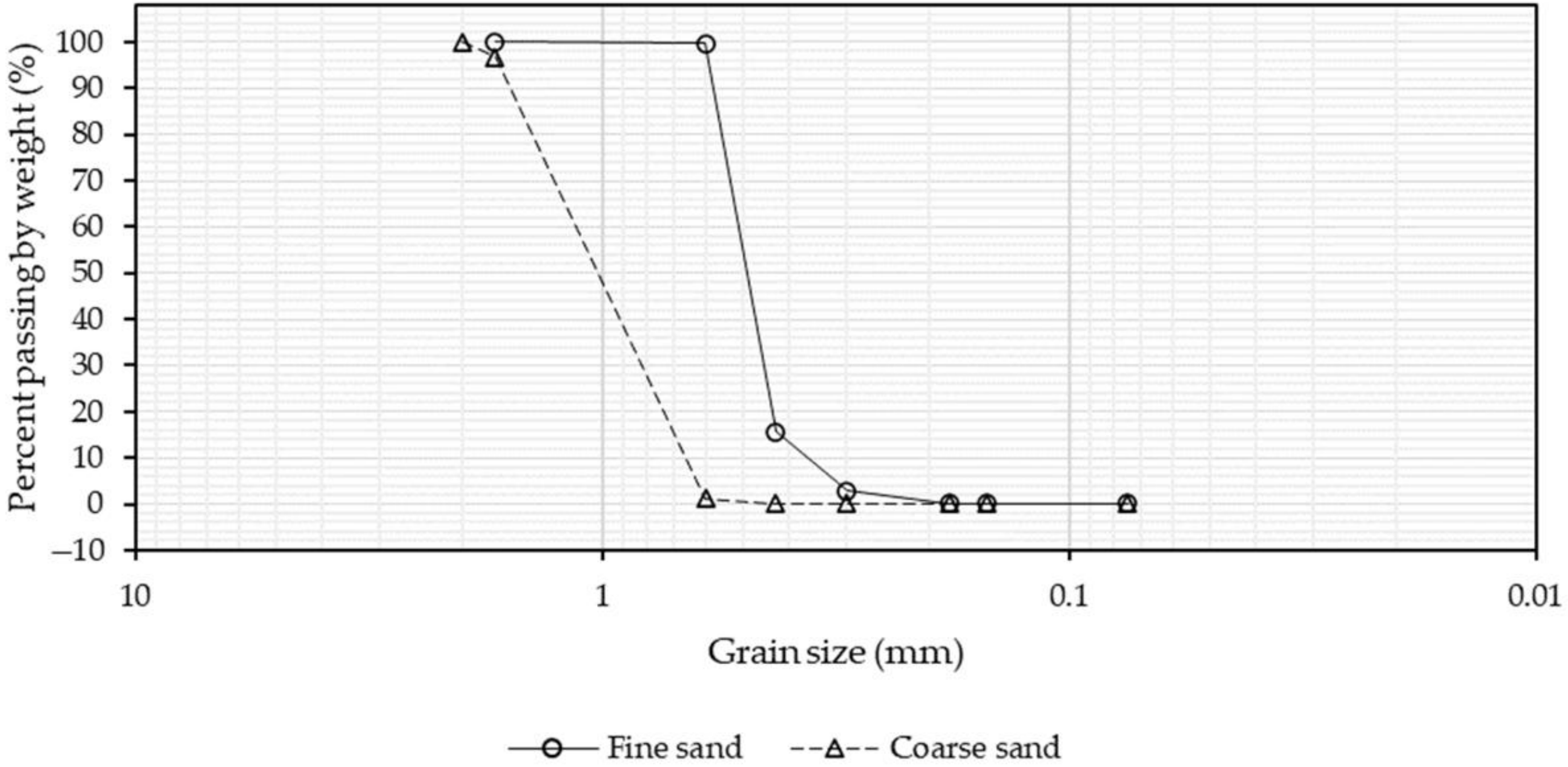

Figure 4. Test soil particle size distributions.

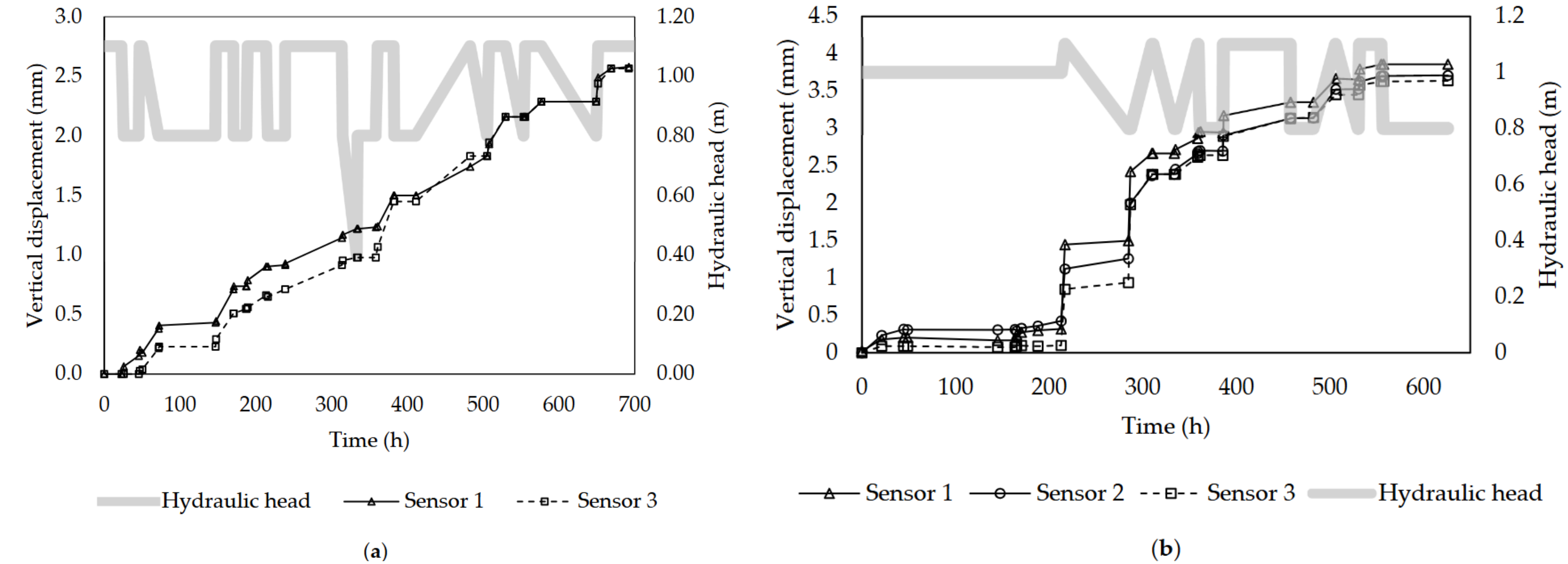

Figure 5. Variation of water table and vertical deformation in coarse sand. (**a**) The first scenario and (**b**) second scenario of coarse sand.

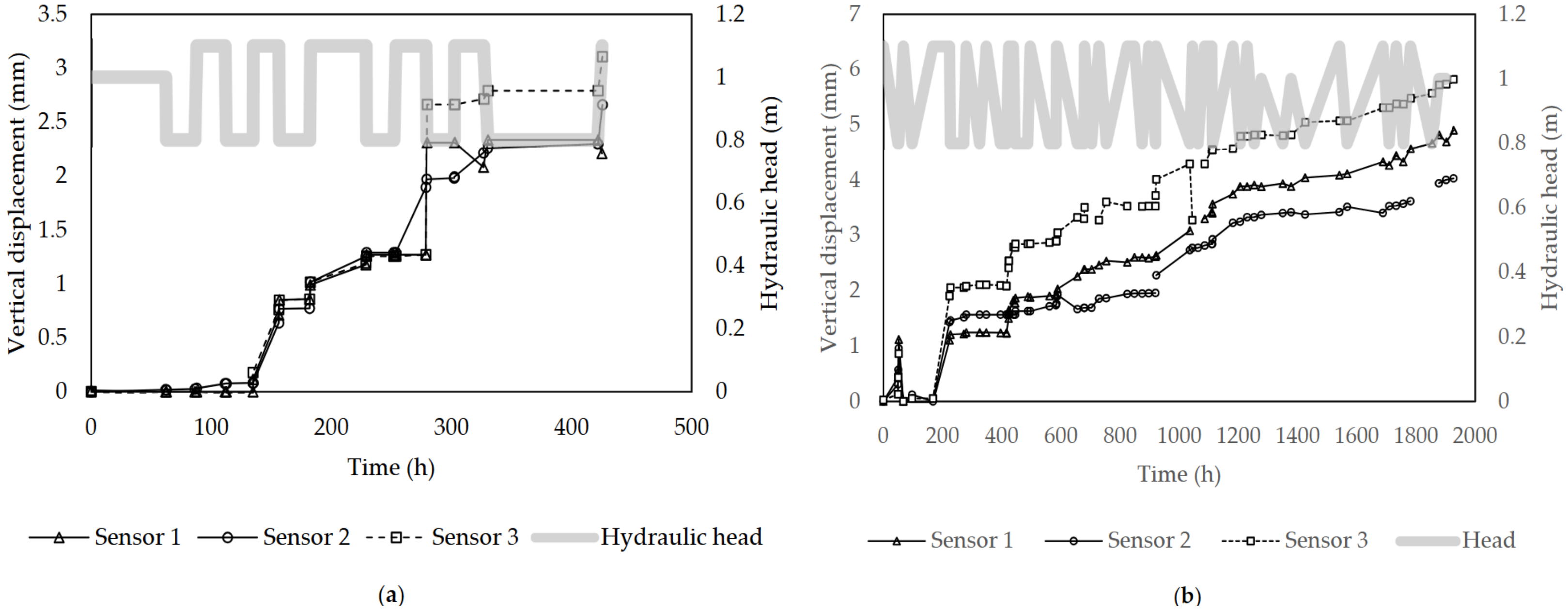

Figure 8. Variation of the water table and vertical deformation for fine sand type 30–40 for the (**a**) first scenario and (**b**) second scenario of fine sand.

Numerical Model

- The **hydraulic head** was a key input parameter to define the variation of the water level in the numerical model.
- The numerical model considered all experimentally acquired data, such as **Initial porosity**、**Hydraulic Conductivity**、 **Soil grain size distribution** by ASTM Standard.
- The resulting vertical displacement obtained by the experimental results was used to compare and calibrate the subsidence results from the numerical model.
- COMSOL Multiphysics 6.0 was used to solve vertical displacement with Terzaghi's law.
- The **specific storage** was selected as the calibration parameter.

假設你在某時間點測到垂直變形（mm）為：

```csharp
[3.1, 3.3, 3.0, 3.2, 3.4]
```

✅ **步驟：**

1. **計算平均值**
   $\bar{x} = \frac{3.1+3.3+3.0+3.2+3.4}{5} = 3.2$
2. **計算標準差（Standard Deviation）**
   $s \approx 0.158$
3. **查 t 值（自由度 df=4，信心水準 95% 時）**
   $t_{0.025,4} \approx 2.776$
4. **計算標準誤（SE）**
   $SE = \frac{s}{\sqrt{n}} = \frac{0.158}{\sqrt{5}} \approx 0.071$
5. **信賴區間公式：**

$$\bar{x} \pm t \cdot SE = 3.2 \pm 2.776 \cdot 0.071 \approx [3.003, 3.397]$$